Theoretical study to optimize the yield of $InGaN/Si$ tandem solar cell using Solcore.

Abdelwahab Douha[a], Benameur Amiri[b,*], Abdelrahmane Belghachi[a]

[a] *University Tahri Mohamed of Bechar, 08.000, Bechar, Algeria*
[b] *University Center NOUR El Bachir, 32.000, El-Bayadh, Algeria*

Abstract

The tandem concept is a potential solution to the Shockley–Queisser limit for single-junction photovoltaic cells. This approach integrates series and parallel interconnections into a junctions configuration, allowing for relaxed material selection and current-matching constraints. The concept has been applied a two-terminal (2T) monolithic tandem solar cell using Indium gallium nitride (InGaN) and thin crystalline silicon (c-Si) as top and bottom cells InGaN/Si . The InGaN cell, with a band-gap of 1.7 eV, is used as the top sub-cell, while the c-Si cell serves as the bottom sub-cell, Optical and electrical properties of InGaN alloys is being intensively studied to be combined with silicon by implementing $SiO_2/Si3N4$ interlayers. Adhesion of nano-interlayer appears to reduce photonic electro-migration hurdle between InGaN and c-Si, in order to achieve high-efficiency solar cell. However, a relatively thick layer of InGaN is difficult to grow due to the relaxation issue in material. This issue can be avoided by eboxy layer. The tandem structure is optimized based on the thickness and doping concentration and performed using the Wien2k and Solcore simulator under standard one Sun (AM1.5G, 1000 W/m2) illumination. We have shown that 54% of In is needed to ensure the current matching between the top cell and the bottom cell. With feasible structural parameters, we have shown that an efficiency near to 30% can be achieved in the optimum tandem.

Keywords: Solcore, Wien2k code, III-Ns, Tandem solar cell, eboxy layer.

*Benameur Amiri

Email addresses: doha@gmail.com (Abdelwahab Douha), lpdsamis@gmail.com (Benameur Amiri), abelghachi@yahoo.fr (Abdelrahmane Belghachi)

1. Introduction

III-Ns semiconductors, including aluminum nitride (AlN), gallium nitride (GaN), and indium nitride (InN), are highly promising building for optoelectronics and high-power electronics [1]. III-Ns have wurtzite crystal structure at ambient conditions, and the direct band-gap changes from 0.7 eV of InN, to 6.2 eV of AlN, are displaying large amount of commercialized optoelectronics devices, including Photodetectors [2, 3, 4], light-emitting diodes (LEDs) ([5, 6, 7], laser diodes (LDs) [8], and solar cells [9, 10, 11],which are applied in energy harvesting. Compared to other semiconductors, III-Ns demonstrate a fundamental advantage of the formation of heterogeneous structures, such as quantum wells, and quantum dots. Heterogeneous structures of III-Ns can be manufactured through key crystal growth techniques, including molecular beam epitaxy (MBE), metal-organic chemical vapor deposition (MOCVD) and hydride vapor-phase epitaxy (HVPE) [12, 13, 14].Due to the inability of a single solar cell to absorb large solar spectrum photons efficiently, multi-junction (tandem) solar cells have been the focus of much theoretical and experimental work in the past few decades. The most successful efforts to date have focused on the use of semiconductors such as II-VI and III-V alloys to construct such cells, achieving energy conversion efficiencies of over 30%. Indium Gallium Nitride (InGaN) range band-gap can be engineered from 0.7 to 3.4 eV, and this makes it suitable for a range of tandem solar cell designs. The tandem cells are able to use high-energy photons more efficiently than those limited to band-gaps of less than 1.8 eV, will also have the advantage that Si is relatively cheap and abundant as well as that the Si range gap of 1.2 eV is ideally suited to the lower connection of a high-efficiency two-link solar cell. The growth of InGaN based opto-electronic device structures on Si has been extensively investigated previously with the goal of optimizing the interface layers between the Si and the active layers to reduce defects in the Ns layers and to improve device performance. Hsu et al.[15] saw at an alloy composition of $In_{0.46}Ga_{0.54}N$, the conduction band of InGaN has the same energy as the valence band of Si, and so a $n - In_{0.46}Ga_{0.54}N/p - Si$ interface should form a low resistance Ohmic junction. Recent studies have shown that high quality InGaN nanostructures can be grown directly on Si substrate [16, 17]. From the analysis, it is found that $In_{0.54}Ga_{0.46}N$ shows the best performance for InGaN/Si solar cell and it seems to be matched with the underneath Si cell current density as series configuration. In this study, we have performed a detailed investigation of the optimize and performance

characterization of $In_{0.54}Ga_{0.46}N/Si$ tandem solar cell.

2. Methode and modelisation

This study used the Solcore simulator to investigate the performance of single junction and tandem solar cells. The simulator solves semiconductor transport equations and Poisson's equation independently through a grid, incorporating physical models into the simulation. Solcore is a multi-scale, modular simulation framework for solar energy research, written in Python. Is evolved from SOL, a Fortran-based, quantum well solar cell solver developed by Nelson and Connelly [18], uses electronic and optical parameters obtained from different sources for a consistent set of electronic and optical properties. In order to calculate and model the optical response of potential solar cell and material systems, Solcore incorporates a resource of freely available optical constant data measured by Sopra S.A. and provided by Spectra Inc.[19]. To calculate the band structure of a material Solcore includes a modified 8-band Pikus–Bir Hamiltonian under biaxial strain, considering the coupling between the conduction, heavy hole, light hole and split-off bands. The eigenfunctions ψ and eigenstates E are the solutions of the following equation, where H is the Pikus–Bir Hamiltonian:

$$\begin{pmatrix} E_{cb} & -\sqrt{3}T & \sqrt{2}U & -U & 0 & 0 & -T^* & -\sqrt{2}T^* \\ & E_{hh} & \sqrt{2}S & -S & 0 & 0 & -R & -\sqrt{2}R \\ & & E_{lh} & -\sqrt{2}Q & T^* & R & 0 & \sqrt{3}S \\ & & & E_{so} & \sqrt{2}T^* & \sqrt{2}R & -\sqrt{3}S & 0 \\ & & & & E_{cb} & -\sqrt{3}T^* & \sqrt{2}U & -U \\ & & & & & E_{hh} & \sqrt{2}S^* & -S^* \\ & & & & & & E_{lh} & -\sqrt{2}Q \\ & & & & & & & E_{so} \end{pmatrix} \Psi = E\Psi$$

To evaluate the realistic optical behavior of a solar cell, and obtain the fraction of incoming light reflected, absorbed, and transmitted as a function of the wavelength of the light and the position inside the structure. it is important to consider the interaction of incident electromagnetic radiation with a succession of both absorbing and non-absorbing planar layers using TMM, The implementation of TMM in Solcore uses the freely available module developed by Byrnes [20]. Solcore includes four solvers to calculate the electrical properties of a single-junction device, these are: detailed balance,

Figure 1: Structure of InGaN/Si tandem solar cell.

2-diode equation, depletion approximation, and Poisson-drift-diffusion. To combine them into a multi-junction device, it is necessary to consider that the individual junctions are electrically connected in series and the potential coupling of light emitted by the wider band-gap junctions into those with smaller band-gap. The solar cell structure we use to model the performance of an InGaN/Si tandem solar cell is shown in Fig.1 The tandem cell consists of InGaN junction grown on top of Si junction. Each junction is composed of a p-type layer grown on top of an n-type layer. " SiN anti-reflection coating on Si that it is more useful to suppress reflection at wavelengths where there are more photons which could be absorbed". The SiO_2 inter-layer is used between the InGaN and Si junction to reduce severe stacking faults or defects between these junctions. The doping concentration for each layer is $5 \times 10^{17} cm^{-3}$ p-InGaN, $5 \times 10^{18} cm^{-3}$ n-InGaN, $6 \times 10^{17} cm^{-3}$ p-Si and $6 \times 10^{17} cm^{-3}$ n-Si. All material parameters used in this optimization are listed in the tab.1.

3. Resultat and Discution

The energy band diagram under the equilibrium condition of the band alignment of $In_{0.54}Ga_{0.46}N$ and Si is illustrated in Fig.2 can be exploited for the fabrication studied structure of tandem $In_{0.54}Ga_{0.46}N/Si$ hetero-junctions solar cells that may have power conversion efficiency. To understand of these hetero-junctions, a band diagram as shown χ_1 and χ_2 are the electron affinities for both materials. Therefore, the conduction band of

Parameters	*Unites*	*GaN*	*InGaN*	*Si*
a	A^o	5.186	...	5.43
χ	eV	4.1	5.44	4.05
E_g	eV	3.42	1.9	1.2
$m*_e$	m_0	0.2	0.07	0.36
$m*_{hh}$	m_0	1.4	0.7	0.81
$m*_{lh}$	m_0	0.3	...	0.16
N_c	cm^{-3}	2.3×10^{18}	...	3.2×10^{19}
N_v	cm^{-3}	4.6×10^{19}	...	1.8×10^{19}
p (N_A)	...	5×10^{17}	...	6×10^{17}
n (N_D)	...	5×10^{17}	...	6×10^{17}
μ_e	$cm^2/(V.s)$	1000	300	1400
μ_h	$cm^2/(V.s)$	350	50	450
D_e	cm^2/s	25	...	...
D_h	cm^2/s	9	...	...
v_e	m/s	2.6×10^5	...	
v_h	m/s	9.4×10^4	...	...
ϵ_0	...	8.9	11.7	11.9
ϵ_∞	...	5.35	...	...
S_n	cm/s	...	1×10^6	1×10^6
Sp	cm/s	...	1×10^6	1×10^6
R_{A_e}	$cm^6 s^1$	...	1.5×10^{-30}	...
R_{A_h}	$cm^6 s^1$	...	1.5×10^{-30}	...
τ_n	ns	...	1	10^3
τ_p	ns	...	1	10^3
τ_{SRH}	ns	...	1×10^{-5}	5×10^{-6}

Table 1: Parameters used in the electrical simulation of InGaN/Si tandem solar cell.

$In_{0.54}Ga_{0.46}N$ is below the conduction band of Si and the valence band of $In_{0.54}Ga_{0.46}N$ lies below the valence band of Si, leading to the formation of a type II hetero-junction.

To include a material not currently present in Solcore's database, or to use measured data instead of literature data base, we need to add the material to the data-base manually. This process requires both the refractive index (n) and extinction coefficient (k) data, as well as a parameter file formatted as file.txt, calculated using Wien2k, which must be placed in Solcore's source files. The Fig.3 and Tab.1 displays the average refractive index $n(\omega)$, extinction coefficient $k(\omega)$, and essential parameters materials properties such as the band-gap, lattice constant, and effective carrier masses, used in optimization. The refractive index $n(\omega)$ and the extinction coefficient $k(\omega)$ play an important role with respect to the electronic and optical properties of materials, as shown in Fig.3, the peaks of refractive index all reside within the visible region and Si was found to have the highest refractive index. The peaks of $n(\omega)$ shift significantly toward lower energies (infrared and visible regions). The static refractive indices n_0) increase from GaN to Si. The extinction coefficient $k(\omega)$ right Fig.3 is related to the decay or damping of the oscillation amplitude of the incident electric field. $k(\omega)$ has similar behavior to the absorption coefficient $\alpha(\omega)$, since they are correlated via the Beer-Lambert law. $k(\omega)$ is seen to vanish at very high frequency due to the weak absorption.

We introduce a new material,InGaN, using input files containing the n and k values in data-base Solcore's. We define our light source as the AM1.5G spectrum, and build the solar cell layer by layer. We also include additional parameters not found in Solcore's materials database, such as minority carrier diffusion lengths. We account for surface recombination velocities, add shading due to cell metallization (estimated at 5%), and consider a finite series resistance. For the final setup, we configure the spacing for each layer, setting it to 0.1 nm for all layers except the final silicon layer, which is set to 10 nm.

After assembling the cell and setting the necessary options, we calculate and plot the External Quantum Efficiency (EQE) and the light IV characteristics. During the Transfer Matrix Method (TMM) calculation, we observe interference fringes and front-surface reflections. We then calculate and plot the light IV under the AM1.5G spectrum, using a purely optical TMM simulation to estimate the photo-generated current in each sub-cell. This helps us determine the required material thicknesses for current-matching.

	$J_{sc}(mA/cm^2)$	V_{oc}(V)	FF (%)	Efficiency (%)
$In_{054}Ga_{0.46}N$	32.94	1.02	87.5	29.02
Si	35.02	0.72	84.9	21.5
$In_{054}Ga_{0.46}N/Si$	34.01	1.62	91.55	29.27
				30.31[21], 35.2[22],
				36.5[23], 37.23[24]

Table 2: Photovoltaic parameters of the top $InGaN$, bottom Si, and tandem $In_{054}Ga_{0.46}N/Si$ cells.

Our goal is to optimize the current of the current-limiting cell in the structure, aiming to maximize the lowest sub-cell current to achieve the highest possible current-matching. Since the differential evolution algorithm minimizes the negative of this current, we use it to find the optimal initial values for total layer thicknesses. We then perform a full electrical simulation to finalize the n-type and p-type layer thicknesses and calculate the maximum achievable efficiency for the two-junction device.

At this stage, we do not optimize the thickness of bottom cell, as from an optical perspective, it should be infinitely thick to maximize absorption. We set the thickness of InGaN layer to 600 nm. Figure 6 (right) shows the absorption in each layer using the optimized thicknesses. With the optical thicknesses optimized, we design the device similarly to the previous optical simulations. We create an object and call the method to calculate the IV characteristics of the devices, with Figure 6 (left) showing the resulting IV curves.

Fig.6 shows the absorption in each layer using the optimized thicknesses. Now that the layer thickness is optimized from an optical point of view, we want to design the device. Once we have good initial values for the total layer thicknesses, we use full electrical simulation to determine the n and p type layer thicknesses to calculate a maximum possible efficiency.

Fig.5 shows the calculated voltage-current curves for the best thickness of an $In_{0.54}Ga_{0.46}N/Si$ tandem cell device. The IV curve looks reasonably good.

Fig.3 shows us the n and k data for the materials used in this tandem solar cell modeling.

From the above Tab.2, it can be said that the $In_{054}Ga_{0.46}N/Si$ tandem solar cell device gives the best efficiency theoretically, it has not yet been

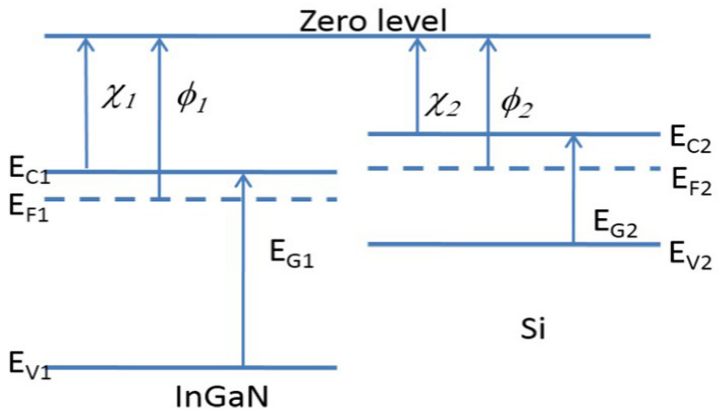

Figure 2: Schematic band diagrams of $InGaN$ and Si before in contact.

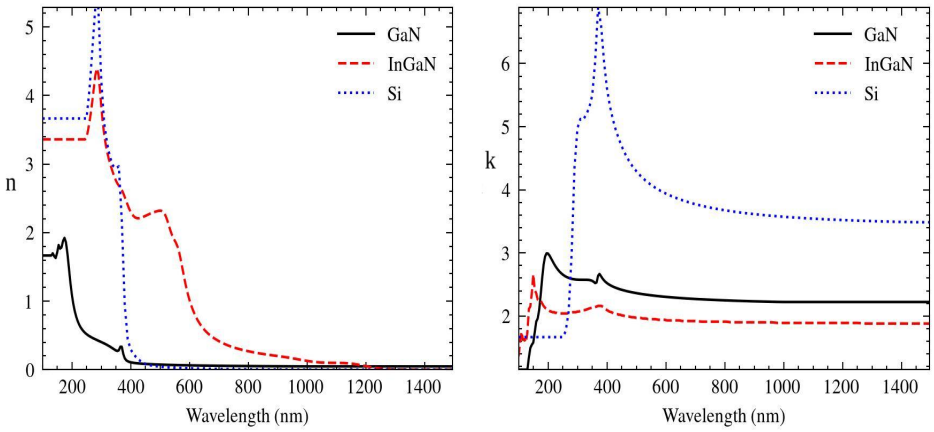

Figure 3: Optical constants of GaN, $In_{0.54}Ga_{0.46}N$ and Si.

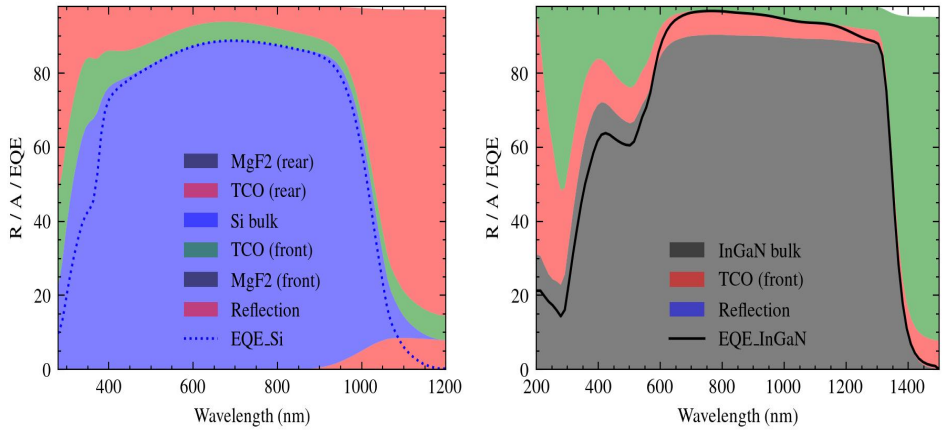

Figure 4: External quantum efficiency yield for each independent cell of Si and $In_{0.54}Ga_{0.46}N$.

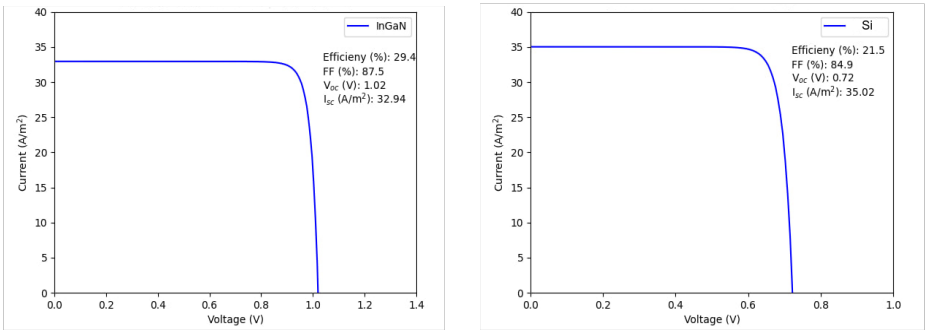

Figure 5: I-V Characteristics of $In_{0.54}Ga_{0.46}N$ and Si Single solar cells.

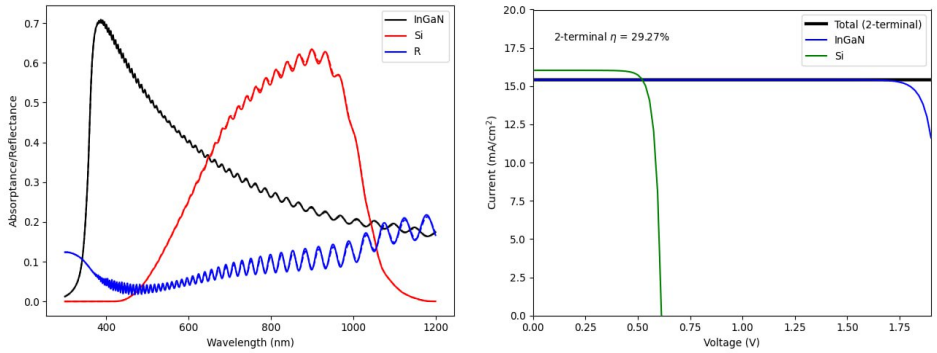

Figure 6: absorption and I-V Characteristics of $In_{0.54}Ga_{0.46}N/Si$ tandem solar cells.

proven due to the intrinsic defects of the cell caused by the high indium content. In this work based on simulation results supported by the electrical and optical characteristics of the device. We found that the addition of 54% In to GaN is promising for use in solar cell where the top cell is matched with the bottom cell. Solar cells can also be enhanced by optimizing not only the doping and thickness of each solar cell layer, but also by adding indium content as well.

4. Conclusion

Using Solcore simulator, we theoretically investigated the potential power conversion efficiencies that can be achieved by a tandem $In_{054}Ga_{0.46}N/Si$ solar cell. There are several limitations such as thickness, band-gap, and lattice constant mismatch that need to be considered. Computational models based on DFT theory and the K.P method can provide insight into photovoltaic solar cells. Behavioral calculations can be performed, through experimental and theoretical parameters such as index coefficient, band gaps and thicknesses. These formulations are able to model the optical and electrical properties of tandem solar cells. We found that the optimal band gap and top layer thickness were **1.8 eV** and **600 nm**, respectively, and achieved an optimal conversion efficiency of 30%, which is higher than that of a single-junction Si solar cell. The obtained results show that an indium content of 54% is optimal for the tandem solar cell where the top cell matches the bottom cell. In content as tandem solar cell is very important in order to optimize the overall performance of solar cell, such as open circuit voltage, short circuit current density, fill factor and quantum efficiency. The stacking defects are minimized by introducing an SiO_2 inter-layer and the current density between the junctions is matched by choosing an appropriate In content.

References

[1] a. S. Strite, H. Morkoç, Gan, aln, and inn: a review, Journal of Vacuum Science & Technology B: Microelectronics and Nanometer Structures Processing, Measurement, and Phenomena 10 (4) (1992) 1237–1266.

[2] C. Pernot, A. Hirano, M. Iwaya, T. Detchprohm, H. Amano, I. Akasaki, Solar-blind uv photodetectors based on gan/algan pin photodiodes, Japanese Journal of Applied Physics 39 (5A) (2000) L387.

[3] Q. Chen, J. Yang, A. Osinsky, S. Gangopadhyay, B. Lim, M. Anwar, M. Asif Khan, D. Kuksenkov, H. Temkin, Schottky barrier detectors on gan for visible–blind ultraviolet detection, Applied Physics Letters 70 (17) (1997) 2277–2279.

[4] E. Munoz, E. Monroy, J. Garrido, I. Izpura, F. Sánchez, M. Sánchez-Garcıa, E. Calleja, B. Beaumont, P. Gibart, Photoconductor gain mechanisms in gan ultraviolet detectors, Applied physics letters 71 (7) (1997) 870–872.

[5] S. Nakamura, M. Senoh, T. Mukai, High-power ingan/gan double-heterostructure violet light emitting diodes, Applied Physics Letters 62 (19) (1993) 2390–2392.

[6] M. Funato, M. Ueda, Y. Kawakami, Y. Narukawa, T. Kosugi, M. Takahashi, T. Mukai, Blue, green, and amber ingan/gan light-emitting diodes on semipolar {11-22} gan bulk substrates, Japanese Journal of Applied Physics 45 (7L) (2006) L659.

[7] K. Iso, H. Yamada, H. Hirasawa, N. Fellows, M. Saito, K. Fujito, S. P. DenBaars, J. S. Speck, S. Nakamura, High brightness blue ingan/gan light emitting diode on nonpolar m-plane bulk gan substrate, Japanese Journal of Applied Physics 46 (10L) (2007) L960.

[8] S. Nakamura, M. Senoh, S.-i. Nagahama, N. Iwasa, T. Yamada, T. Matsushita, H. Kiyoku, Y. Sugimoto, T. Kozaki, H. Umemoto, et al., Continuous-wave operation of ingan/gan/algan-based laser diodes grown on gan substrates, Applied Physics Letters 72 (16) (1998) 2014–2016.

[9] C. J. Neufeld, N. G. Toledo, S. C. Cruz, M. Iza, S. P. DenBaars, U. K. Mishra, High quantum efficiency ingan/gan solar cells with 2.95 ev band gap, Applied Physics Letters 93 (14) (2008).

[10] O. Jani, I. Ferguson, C. Honsberg, S. Kurtz, Design and characterization of gan/ ingan solar cells, Applied Physics Letters 91 (13) (2007).

[11] C. Jiang, L. Jing, X. Huang, M. Liu, C. Du, T. Liu, X. Pu, W. Hu, Z. L. Wang, Enhanced solar cell conversion efficiency of ingan/gan multiple quantum wells by piezo-phototronic effect, ACS nano 11 (9) (2017) 9405–9412.

[12] S. Jain, M. Willander, J. Narayan, R. V. Overstraeten, Iii–nitrides: Growth, characterization, and properties, Journal of Applied Physics 87 (3) (2000) 965–1006.

[13] S. Yoshida, S. Misawa, S. Gonda, Properties of al x ga1- x n films prepared by reactive molecular beam epitaxy, Journal of Applied Physics 53 (10) (1982) 6844–6848.

[14] D.-B. Li, M. Aoki, T. Katsuno, H. Miyake, K. Hiramatsu, T. Shibata, Influence of growth conditions on al incorporation to alxga1- xn (x> 0.4) grown by movpe, Journal of crystal growth 298 (2007) 372–374.

[15] L. Hsu, W. Walukiewicz, Modeling of ingan/si tandem solar cells, Journal of Applied Physics 104 (2) (2008).

[16] S. Arafin, X. Liu, Z. Mi, Review of recent progress of iii-nitride nanowire lasers, Journal of Nanophotonics 7 (1) (2013) 074599–074599.

[17] Y. Wang, S. Vanka, J. Gim, Y. Wu, R. Fan, Y. Zhang, J. Shi, M. Shen, R. Hovden, Z. Mi, An in0. 42ga0. 58n tunnel junction nanowire photocathode monolithically integrated on a nonplanar si wafer, Nano Energy 57 (2019) 405–413.

[18] J. Connolly, Analytical models of bulk and quantum well solar cells and relevance of the radiative limit., in: Y. M. Fara, L. (Ed.), Advanced Solar Cell Materials, Technology, Modelling, and Simulation, chap. 5, PA, IGI Global, Hershey, 2013, p. 59–77.

[19] S. Sopra, Optical data from sopra sa, Available at h ttp://www. sspectra. com/sopra. html (2008).

[20] S. J. Byrnes, Multilayer optical calculations, arXiv preprint arXiv:1603.02720 (2016).

[21] L. Hsu, W. Walukiewicz, Modeling of ingan/si tandem solar cells, Journal of Applied Physics 104 (2) (2008).

[22] Z. Li, H. Xiao, X. Wang, C. Wang, Q. Deng, L. Jing, J. Ding, X. Hou, Theoretical simulations of ingan/si mechanically stacked two-junction solar cell, Physica B: Condensed Matter 414 (2013) 110–114.

[23] S.-W. Feng, C.-M. Lai, C.-Y. Tsai, L.-W. Tu, Numerical simulations of the current-matching effect and operation mechanisms on the performance of ingan/si tandem cells, Nanoscale Research Letters 9 (2014) 1–10.

[24] S. M. Ahmadi, F. Parandin, Design and simulation of a highly efficient ingan/si double-junction solar cell, Journal of Electrical and Computer Engineering Innovations (JECEI) 5 (2) (2017) 157–162.